NMR Evidence of Spin Supersolid and Pomeranchuk Effect Behaviors in Triangular-Lattice Antiferromagnet $Rb_2Ni_2(SeO_3)_3$

Ying Chen(陈颖)[1†], Zhanlong Wu(吴占龙)[1†], Xuejuan Gui(桂雪娟)[1†], Guijing Duan(段桂靖)[1†], Shuo Li(李硕)[2], Xiaoyu Xu(徐霄宇)[1], Kefan Du(杜柯帆)[1], Xinyu Shi(史昕雨)[1], Rui Bian(边蕊)[1], Xiaohui Bo(薄晓慧)[1], Guochen Liu(刘国宸)[1], Jun Luo(罗军)[2], Jie Yang(杨杰)[2], Yi Cui(崔祎)[1,3*], Rui Zhou(周睿)[2*], Jinchen Wang(汪晋辰)[1,3*], Rong Yu(俞榕)[1,3*], and Weiqiang Yu(于伟强)[1,3*]

[1]*Department of Physics and Beijing Key Laboratory of Opto-electronic Functional Materials & Micro-nano Devices, Renmin University of China, Beijing 100872, China*

[2]*Institute of Physics, Chinese Academy of Sciences, and Beijing National Laboratory for Condensed Matter Physics, Beijing 100190, China*

[3]*Key Laboratory of Quantum State Construction and Manipulation (Ministry of Education), Renmin University of China, Beijing 100872, China*

(Received 16 January 2026; accepted manuscript online 10 March 2026)

We perform ^{85}Rb nuclear magnetic resonance (NMR) measurements on the $S = 1$ bilayer triangular-lattice antiferromagnet $Rb_2Ni_2(SeO_3)_3$ in magnetic fields up to 26 T. In the field range from 3 to 26 T, the NMR spectral lines split, and their respective spectral weight ratios reveal the existence of the magnetic up-up-down (UUD) phase, although the 1/3-plateau phase is only attained in fields above 16 T. Two distinct gapless regimes are further identified: one at low fields and low temperatures, and the other at high fields and high temperatures, which are consistent with spin supersolid Y and V phases. Notably, the UUD-V phase boundary exhibits a negative slope in $\mathrm{d}T/\mathrm{d}H$, where the supersolid phase is located at temperatures above those of the solid phase because of strong low-energy spin fluctuations.

DOI: 10.1088/0256-307X/43/4/040709 CSTR: 32039.14.0256-307X.43.4.040709

Introduction. Frustrated systems exhibit various novel physical properties owing to their macroscopic degeneracy.[1–7] Triangular-lattice antiferromagnets (TLAFMs) are a representative example and have been extensively investigated in both the quantum and classical regimes.[8–13] They provide a versatile platform for investigating novel phenomena, including magnetic plateaus,[14–16] quantum spin liquids,[17–20] and spin supersolids (SS).[21–23] Furthermore, these phases are highly sensitive to and can be tuned by various perturbations, such as spin anisotropy, longer-range interactions, magnetic fields, impurities, and lattice deformations, owing to the relationship between thermal and quantum fluctuations.[9,12,24–28] As a unique quantum state, the SS extends the original concept of supersolids[29] to magnetic systems. This arises from the spontaneous breaking of both spin rotational and lattice symmetries, and is characterized as a planar order coupled to an up-up-down (UUD) spin pattern in TLAFMs. Experimental evidence of spin supersolidity has only been reported in several $S = 1/2$ triangular-lattice compounds, such as $Na_2BaCo(PO_4)_2$,[30–32] $K_2Co(SeO_3)_2$,[33,34] and $Rb_2Co(SeO_3)_2$.[35]

Recently, a class of bilayer triangular-lattice materials has received significant attention.[36–42] In these systems, the relationship between intralayer geometric frustration and interlayer couplings enhances quantum fluctuations, thus resulting in emergent critical behaviors under magnetic fields, such as the Kawamura universality class,[36,43] the Potts criticality,[37,44] and Berezinskii–Kosterlitz–Thouless phase transitions,[38] as well as candidate quantum spin liquids,[39] which extend beyond the typical frameworks of antiferromagnets. An open and intriguing question is whether exotic phases can emerge in $S = 1$ TLAFMs. In this regard, the Ising anisotropic bilayer TLAFM $K_2Ni_2(SeO_3)_3$ with weak bilayer interactions[41] offers a case study to address this question. It not only exhibits a 1/3-like magnetization plateau between 18 and 26 T[42] but also shows double magnetic transition lines in both magnetic-susceptibility and heat-capacity measurements.[41,42] These features resemble those observed in easy-axis anisotropic TLAFMs and suggest the stabilization of the UUD and SS phases.[8]

Herein, we report the NMR measurements of $Rb_2Ni_2(SeO_3)_3$, which is an isostructural compound of $K_2Ni_2(SeO_3)_3$, in fields up to 26 T. The main results are

†These authors contributed equally to this work.
*Corresponding authors. Email: cuiyi@ruc.edu.cn; rzhou@iphy.ac.cn; jcwang_phys@ruc.edu.cn; rong.yu@ruc.edu.cn; wqyu_phy@ruc.edu.cn

© 2026 Chinese Physical Society and IOP Publishing Ltd. All rights, including for text and data mining, AI training, and similar technologies, are reserved.

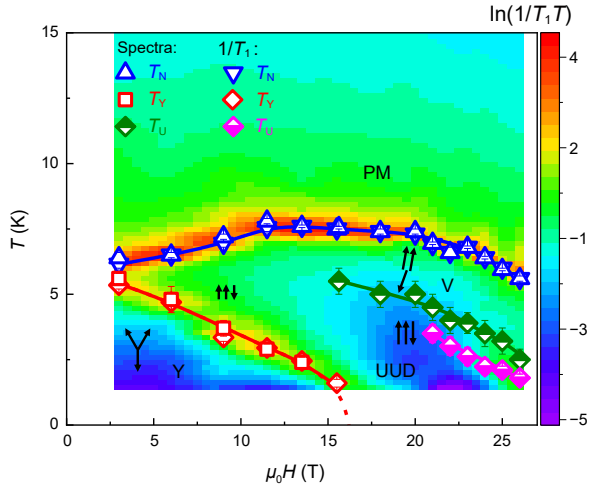

Fig. 1. Phase diagram of $Rb_2Ni_2(SeO_3)_3$. Heat map represents contour plot of $1/T_1T$ data. T_N, T_Y, and T_U represent phase boundaries among PM, UUD, Y, and V phases, respectively, which are determined from spectral and spin-lattice relaxation rate data. Solid and dotted lines provide visual guidance.

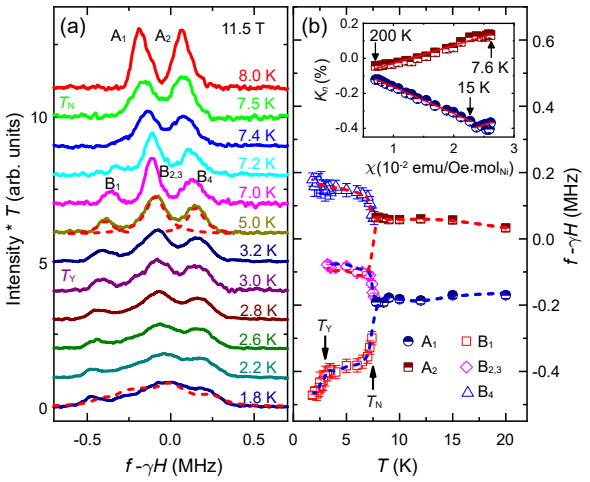

Fig. 2. Low-field NMR spectra. (a) ^{85}Rb center lines measured at 11.5 T under decreasing temperatures. Vertical data offsets are applied for clarity. A_1 and A_2 are two peaks observed at and above 7.5 K; and B_1, $B_{2,3}$, and B_4 represent peaks resolved at lower temperatures. A three-Lorentzian fit is applied to the data at 5 K, with the relative spectral weight fixed at a ratio of 1:3:2. Simulated spectrum of Y phase is plotted at 1.8 K (see text). (b) Frequencies of all resolved peaks as a function of temperature. T_N and T_Y denote transition temperatures determined from frequency change in peaked spectra. Dashed lines provide visual guidance. Inset: High-temperature K_n of A_1 and A_2 plotted against magnetic susceptibility. Solid straight lines represent linear function fits to data for obtaining the hyperfine coupling constant (see text).

summarized in the phase diagram in Fig. 1, which is overlaid on the spin-lattice relaxation rate data $1/T_1$. A dome-shaped Néel transition T_N was determined from both the NMR line splitting and the peaks in $1/T_1$. Below T_N, we resolved two additional transition lines at T_Y and T_U. Our spectral analysis in the intermediate region intercepting the T_Y and T_U lines revealed the UUD phase, although the 1/3-magnetization plateau phase was only achieved in fields above 16 T.[42] Gapless behavior was observed below the T_Y line and above the T_U line, thus providing strong evidence of two SS phases. Remarkably, the V-UUD phase boundary exhibited a negative slope dT/dH, thus signifying a counterintuitive transition from a low-symmetry phase to a high-symmetry phase upon cooling. This observation is consistent with the magnetic analogue of the Pomeranchuk effect.[45–48] Our study elucidates novel emergent quantum phenomena in $S = 1$ bilayer antiferromagnets.

Low-Field NMR Spectra and Double Phase Transitions. The detailed materials and measurement techniques are described in the Supplementary Materials (SM).[49] The central NMR lines of ^{85}Rb are shown in Fig. 2(a) at different temperatures under a low field of 11.5 T.

A_1 and A_2, which exhibit a spectral weight ratio of approximately 1:1, were resolved. They are attributed to two inequivalent ^{85}Rb sites caused by random half-occupied Se(II) ions (see Section S1 of the SM[49]).

Below 7.5 K, both lines split: A_1 split into two peaks labeled B_1 and B_3, whereas A_2 split into B_2 and B_4. Since B_2 and B_3 overlapped, only three peaks were observed. This line splitting indicates a phase transition from the paramagnetic (PM) state to a symmetry-breaking state upon cooling. Below 3 K, the spectra exhibited significant broadening, thus rendering it difficult to resolve peaks B_2 and B_3, whereas B_1 and B_4 remained resolvable. Subsequently, the frequencies of the respective peaks were obtained and plotted as a function of temperature, as shown in Fig. 2(b). The calculated Knight shifts $K_n(T)$ for A_1 and A_2 at high temperatures are plotted against the magnetic susceptibility $\chi(T)$ in the inset of Fig. 2(b), with temperature as an implicit variable. Using linear fits, the hyperfine coupling constants were obtained as $A_{hf} = 0.057(2)$ T/μ_B for A_2, and $A_{hf} = -0.085(1)$ T/μ_B and $A_{hf} = 0.062(2)$ T/μ_B for A_1 at temperatures above and below 15 K, respectively.

Below 7.5 K, the frequencies of $B_{2,3}$ and B_4 increased significantly and then plateaued, whereas that of B_1 decreased significantly before stabilizing. Below 3 K, the frequencies of B_1 (B_4) exhibited a kinked decrease (increase) upon further cooling. These changes in the spectra clearly indicate two successive phase transitions upon cooling, i.e., at $T_N = 7.5$ K and $T_Y = 3$ K, which correspond to the PM-UUD and UUD-Y phase transitions, respectively, as will be substantiated below.

The spectrum at 5 K was fitted using a three-Lorentzian function, as shown in Fig. 2(a). The fit yielded a relative spectral weight ratio of approximately 1:3:2 from left to right. This distribution is consistent with the UUD phase, considering the two inequivalent ^{85}Rb sites. The UUD spin configuration, which featured two up spins and one down spin, predicted a 1:2 spectral weight ratio for each ^{85}Rb site. The observed 1:3:2 ratio is attributable to the accidental overlap of one peak from each ^{85}Rb site (B_2 and B_3), as supported by the simulated spectra presented in Section S3 of the SM.[49]

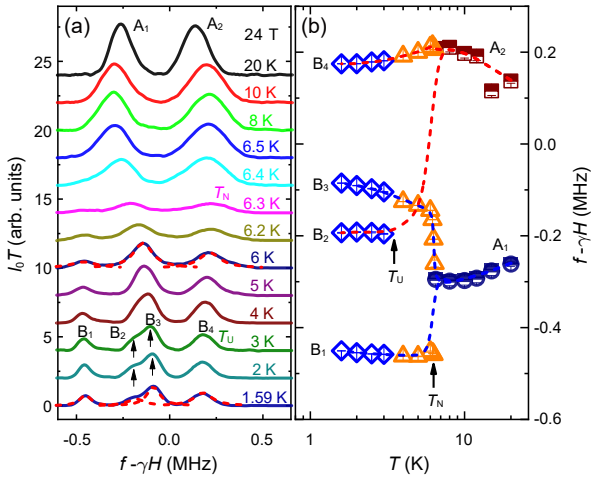

Fig. 3. High-field NMR spectra. (a) Spectra at 24 T under decreasing temperatures. Data are shifted vertically for clarity. B_1 to B_4 indicate peaks resolved at low temperatures. Dashed lines represent three-Lorentzian function fits applied to data at 6 K with fixed a spectral weight ratio of 1:3:2 from left to right, and four-Lorentzian function fits to data at 1.59 K with a fixed ratio of 1:1:2:2. (b) Resonance frequencies of respective spectral peaks measured at 24 T as a function of temperature. Dash lines provide visual guidance.

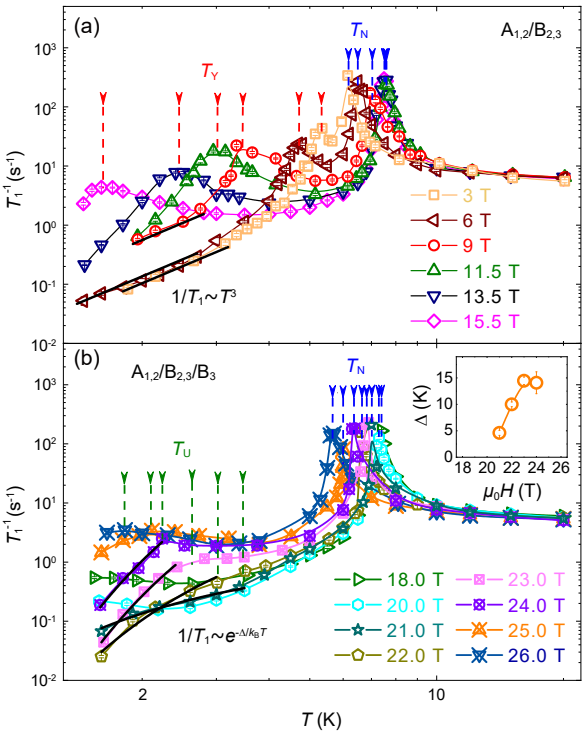

Fig. 4. Spin-lattice relaxation rates. (a) Low-field $1/T_1$ data as a function of temperature. Blue and red arrows indicate peak positions labeled by T_N and T_Y, respectively. Solid straight lines provide visual guidance to power-law scaling $1/T_1 \sim T^3$. (b) High-field $1/T_1$ as a function of temperature. Blue and green arrows denote peak and hump positions labeled by T_N and T_U, respectively. Solid lines represent empirical function fits to $1/T_1 \sim e^{-\Delta/k_BT}$ with energy gap Δ. Inset: Δ as a function of field.

Additionally, we performed a spectral analysis on the data at 1.8 K (Fig. S3 in the SM [49]) and discovered that good agreement between the simulated and measured data was achieved only when the system was assumed to be in the Y phase [Fig. 2(a)], i.e., when both the in- and out-of-plane orders contributed to line splitting via a dipolar-type hyperfine coupling to the ligand sites. The spectrum shows significant broadening of each line compared with that above 3 K, thus indicating a change in the magnetic structure from UUD to the supersolid Y phase with the development of the in-plane AFM order. Gapless excitations, which further support the supersolid nature, were confirmed by the power-law temperature dependence of the $1/T_1$ data, as will be discussed below. Transition temperatures T_Y and T_N determined from the spectra for fields up to 15.6 T are indicated in the phase diagram shown in Fig. 1.

High-Field Spectra and Successive Phase Transitions. Figure 3(a) shows the spectra measured at a high field of 24 T. Two NMR lines due to inequivalent ^{85}Rb sites were observed in the PM phase above 6.3 K. Upon cooling, a three-peak feature developed, thus indicating the onset of magnetic ordering. Below 4 K, a four-peak feature was resolved. Subsequently, the corresponding frequencies of these peaks were plotted as a function of temperature [see Fig. 3(b)]. Two magnetic transitions corresponding to significant frequency changes were identified at $T_N = 6.3$ K and $T_U = 3.5$ K, respectively.

The determined T_N and T_U values are summarized in the phase diagram shown in Fig. 1. Here, T_U can be regarded as the transition temperature from the supersolid V phase to the UUD phase upon cooling. To verify this hypothesis, we examined the low-temperature spectra shown in Fig. 3(a). The spectrum at 6 K reflects a three-Lorentzian function fit with a spectral ratio of 1:3:2 for peaks from left to right, thus suggesting the breaking of the c-axis lattice symmetry in a manner similar to that in the UUD phase. Upon cooling below approximately 3 K, the spectrum split into four peaks, with A_1 splitting into B_1 and B_3, and A_2 splitting into B_2 and B_4. The split spectrum can be fitted using a four-Lorentzian function with a spectral weight ratio of approximately 1:1:2:2, as shown in the 1.59 K data in Fig. 3(a). This is consistent with the UUD phase, where B_3 (B_1) and B_4 (B_2) represent the contributions from the up (down) spins with a population ratio of 2:1.

Our spectral simulations further confirmed that the three-peak spectra between 3 and 6 K agreed well with the V phase [Fig. S3(g) in the SM [49]], whereas the four-peak feature was consistent with the UUD phase with an enhanced staggered magnetic moment compared with the low-field data (Fig. S4 in the SM [49]). In fact, the $1/T_1$ data shown below resolved gapless excitations at temperatures between T_N and T_U and a gapped excitation at temperatures below T_U. Therefore, T_N and T_U can be regarded as successive phase transitions from the PM to the supersolid V phase, and then to the magnetic UUD phase.

Spin-Lattice Relaxation Rate. Low-energy spin fluctuations were examined based on $1/T_1$. Figures 4(a) and 4(b) show the temperature dependence of $1/T_1$ at low and high fields, respectively, as measured on different spectral

peaks defined in Figs. 2 and 3. Notably, $1/T_1$ on A_1 is identical to that on A_2.

At low fields, as the temperature decreased from 20 to 10 K, $1/T_1$ increased gradually, thus indicating the onset of low-energy spin fluctuations. Meanwhile, below 10 K, $1/T_1$ increased significantly and formed a sharp peak at T_N. This signifies the onset of spin fluctuations as the system approached magnetic ordering. Upon further cooling, a broad peak was observed at a lower temperature T_Y, thus indicating the emergence of a second magnetic transition. Subsequently, T_N and T_Y determined from the $1/T_1$ data were added to the phase diagram (Fig. 1), which were consistent with those determined from the NMR spectra. Below T_Y, $1/T_1$ decreased gradually with decreasing temperature and showed power-law behavior $1/T_1 \sim T^3$ for fields between 3 and 9 T. This power-law temperature dependence is indicative of gapless excitations associated with the broken in-plane continuous symmetry of the supersolid Y phase.[31]

At high fields, $1/T_1$ increased upon cooling and developed a sharp peak at T_N. Below T_N, $1/T_1$ decreases rapidly and stabilized over a broad temperature range. Subsequently, it formed a hump at a lower temperature, denoted by T_U. Subsequently, T_N and T_U determined from $1/T_1$ were added to the phase diagram in Fig. 1. T_N determined from $1/T_1$ agreed well with those determined from the spectra. However, T_U determined from $1/T_1$ was slightly lower than that determined from the spectra. In particular, the absence of critical behavior in $1/T_1$ at T_U suggests that the V–U phase transition is a first-order type.

For $T < T_U$, $1/T_1$ decreased rapidly and reflected thermal activation behavior $1/T_1 = ae^{-\Delta/k_B T}$. The gap Δ extracted from the function fit in different fields is summarized in the inset of Fig. 4(b). Δ increased with the field and reached a maximum of 15 K at 23 T. This large gap provides strong evidence for the stabilization of the UUD phase in the high- and low-temperature regimes. By contrast, $1/T_1$ decreased gradually over a wide temperature regime between T_N and T_U across all measured fields. This suggests strong low-energy spin fluctuations in this intermediate-temperature regime, thus implying the emergence of low-lying excitations contributing to magnetic entropy.

Notably, our analysis shows that the NMR spectra in this regime are consistent with those of the supersolid V phase. Combining this with the Ising anisotropy of the system,[41] the gapless excitations provide compelling evidence for the supersolid V phase originally proposed for TLAFMs.[12]

Phase Diagram and Discussions. Using the data presented above, we constructed a complete magnetic phase diagram comprising PM, UUD, Y, and V phases. To understand the nature of the phases precisely, the phase diagram was overlaid on top of the colored contour map of $1/T_1T$ in Fig. 1. A single dome in T_N is shown as a function of the field, which was consistently determined from both spectral splitting and the sharp peak in $1/T_1$. The T_Y and T_U lines were separated and almost parallel to each other, thus enclosing the UUD phase within an intermediate (H, T) regime. Notably, in addition to the lattice symmetry breaking and gapless excitations identified from current NMR measurements, signatures from other probes, such as the pseudo-Goldstone mode—a gap arising from the out-of-plane order but reduced by the interplay with the in-plane order[33]—is desirable for fully characterizing the SS phase in the current compound.

The T_N line is consistent with that reported for the isostructural compound $K_2Ni_2(SeO_3)_3$ (up to 9 T),[41] and $Rb_2Ni_2(SeO_3)_3$ shows a much stronger suppression of T_Y with a magnetic field.

The staggered magnetization from 2.5 to 6 K, as calculated from the NMR line splitting, increased with the field up to 16 T and then stabilized (see Fig. S4 in the SM[49]). Although the magnetic structure reflected the UUD pattern at fields below 16 T, the staggered moment remained low. This indicates the existence of strong fluctuations in the low-field UUD phase, as supported by the absence of gapped behavior at temperatures between T_N and T_Y [see $1/T_1$ data in Fig. 4(a)]. The magnetic plateau phase, as characterized by gapped behavior [Fig. 4(b)], was achieved only in fields above 18 T, which is consistent with the reported 1/3 magnetic plateau.[42]

As summarized in Fig. 1, the characteristic temperature T_U determined from $1/T_1$ increased from 1.8 K at 26 T to approximately 3.5 K at 21 T and eventually vanished near 20 T. The absence of a sharp peak across T_U suggests a first-order transition. This conclusion is further strengthened by the slight discrepancy in T_U determined from the spectral and $1/T_1$ measurements, which indicates a distribution of time scales in the spin dynamics that manifests differently across the different experimental probes.

Additionally, our phase diagram revealed that the supersolid V phase stabilized at higher temperatures, as compared with the UUD phase. This behavior is counterintuitive and, to the best of our knowledge, unique among TLAFMs because the naive expectation is that a phase with more broken symmetries (the V phase, breaking both spin U(1) and lattice C_3 symmetries) would be stabilized at a lower temperature compared with that with fewer broken symmetries (the UUD phase, breaking only the C_3 symmetry). A similar cooling-induced symmetry recovery is the Pomeranchuk effect reported for a ^{3}He system under pressure, where the ordered solid phase appears at temperature higher than that of the liquid phase because of the higher nuclear spin entropy in the solid phase.[45–47] However, the Pomeranchuk effect refers to an entropy-driven mechanism arising from two distinct degrees of freedom,[45–48] whereas the current observation, although in a pure spin system, represents an extension of the concept arising from the competition between the out-of-plane and in-plane orders in frustrated Ising magnets.

To understand the manner by which the physics analogous to the Pomeranchuk effect manifests in our magnetic system, we examined the entropy in the UUD and V phases. Typically, $\Delta S < 0$ is expected with an increase in spin polarization induced by the field. However, the

UUD phase comprised a hard gap Δ; its low-temperature entropy increased as $S_{\rm U} \propto {\rm e}^{-\Delta/T}$, whereas the Goldstone mode associated with the broken spin $U(1)$ symmetry in the supersolid V phase provided the entropy $S_{\rm V} \propto T^2$. Thus, we expect $\Delta S = S_{\rm V} - S_{\rm U} > 0$ at low temperatures. In other words, the subtle relationship between quantum and thermal fluctuations results in a larger entropy in the more ordered V phase. In the experiment, the stable behavior in $1/T_1$ over a large temperature range above $T_{\rm U}$ indicates strong spin fluctuations originating from the high entropy in the V phase. Across the first-order UUD-to-V transition, the Clausius–Clapeyron relationship predicts ${\rm d}T/{\rm d}H = -\Delta M/\Delta S$. Because ΔM is always positive as the magnetic field increases, $\Delta S > 0$ immediately results in ${\rm d}T/{\rm d}H < 0$, which corresponds to the negative slope of the UUD-to-V phase boundary in the H–T diagram, as observed experimentally (Fig. 1). The analysis above is further supported by our theoretical modeling presented in the SM.[49]

Although our NMR data and theoretical model strongly support the entropy-driven mechanism for the negative-slope phase boundary, we must perform high-field specific heat measurements to conclusively establish the magnetic Pomeranchuk effect in this system. The large-entropy effect associated with the Pomeranchuk effect may result in a significant magnetocaloric effect, thus offering potential applications in magnetic refrigeration.

Summary. In summary, we investigated field-induced phases and the related phase transitions in an $S = 1$ bilayer TLAFM $Rb_2Ni_2(SeO_3)_3$ via NMR experiments in longitudinal fields up to 26 T. We established the existence of the UUD phase in an intermediate temperature and field regime, and two supersolid phases (denoted as Y and V) surrounding the UUD phase at low and high fields, respectively. Additionally, the UUD phase survived at low fields but with strong quantum fluctuations before reaching the gapped 1/3-magnetization plateau phase. The V phase appeared at a higher temperature than the UUD phase and exhibited a negative ${\rm d}T/{\rm d}H$ phase boundary. Such a negative slope and the existence of strong low-energy spin fluctuations in the V phase provide compelling evidence for an entropy-driven Pomeranchuk effect. Our results provide important insights into the effect of the relationship between quantum and thermal fluctuations on the emergent quantum states in frustrated spin-1 antiferromagnets.

Acknowledgements. This study was supported by the National Key Research and Development Program of China (Grant Nos. 2023YFA1406500 and 2024YFA1409200), the National Natural Science Foundation of China (Grant Nos. 12374156, 12134020, 12334008, 12374142, and 12304170), the Scientific Research Innovation Capability Support Project for Young Faculty (Grant No. ZYGXQNJSKYCXNLZCXM-M26), the National Key Research and Development Projects of China (Grant No. 2022YFA1403402), and the Strategic Priority Research Program of the Chinese Academy of Sciences (Grant No. XDB1270100). This study was supported by the Synergetic Extreme Condition User Facility (https://cstr.cn/31123.02.SECUF).

References

[1] Brassington A, Huang Q, Aczel A A, and Zhou H D 2024 *Phys. Rev. Mater.* **8** 014005
[2] Kohama Y, Ishikawa H, Matsuo A, Kindo K, Shannon N, and Hiroi Z 2019 *Proc. Natl. Acad. Sci.* **116** 10686
[3] Starykh O A 2015 *Rep. Prog. Phys.* **78** 052502
[4] Yosefin M and Domany E 1985 *Phys. Rev. B* **32** 1778
[5] Derrida B, Vannimenus J, and Pomeau Y 1978 *J. Phys. C: Solid State Phys.* **11** 4749
[6] Cui Y, Yu R, and Yu W 2025 *Chin. Phys. Lett.* **42** 047503
[7] Zhou Y Z, Han X, Luo J, Wu D T, Fang A F, Shen B, Feng B J, Shi Y G, Yang J, and Zhou R 2025 *Chin. Phys. Lett.* **42** 037303
[8] Kawamura H and Miyashita S 1985 *J. Phys. Soc. Jpn.* **54** 4530
[9] Yoshikawa S, Okunishi K, Senda M, and Miyashita S 2004 *J. Phys. Soc. Jpn.* **73** 1798
[10] Seabra L, Momoi T, Sindzingre P, and Shannon N 2011 *Phys. Rev. B* **84** 214418
[11] Nakayama G, Hara S, Sato H, Narumi Y, and Nojiri H 2013 *J. Phys.: Condens. Matter* **25** 116003
[12] Yamamoto D, Marmorini G, and Danshita I 2014 *Phys. Rev. Lett.* **112** 127203
[13] Götze O, Richter J, Zinke R, and Farnell D 2016 *J. Magn. Magn. Mater.* **397** 333
[14] Chubukov A V and Golosov D I 1991 *J. Phys.: Condens. Matter* **3** 69
[15] Farnell D J J, Zinke R, Schulenburg J, and Richter J 2009 *J. Phys.: Condens. Matter* **21** 406002
[16] Susuki T, Kurita N, Tanaka T, Nojiri H, Matsuo A, Kindo K, and Tanaka H 2013 *Phys. Rev. Lett.* **110** 267201
[17] Balents L 2010 *Nature* **464** 199
[18] Balz C, Lake B, Reuther J, Luetkens H, Schönemann R, Herrmannsdörfer T, Singh Y, Nazmul Islam A, Wheeler E M, Rodriguez-Rivera J A, Guidi T, Simeoni G G, Baines C, and Ryll H 2016 *Nat. Phys.* **12** 942
[19] Banerjee A, Lampen-Kelley P, Knolle J *et al.* 2018 *npj Quant. Mater.* **3** 8
[20] Clark L, Sala G, Maharaj D D, Stone M B, Knight K S, Telling M T, Wang X, Xu X, Kim J, Li Y, Cheong S W, and Gaulin B D 2019 *Nat. Phys.* **15** 262
[21] Wang F, Pollmann F, and Vishwanath A 2009 *Phys. Rev. Lett.* **102** 017203
[22] Jiang H C, Weng M Q, Weng Z Y, Sheng D N, and Balents L 2009 *Phys. Rev. B* **79** 020409
[23] Heidarian D and Paramekanti A 2010 *Phys. Rev. Lett.* **104** 015301
[24] Murtazaev A, Badiev M, Ramazanov M, and Magomedov M 2021 *Phase Trans.* **94** 394
[25] Chanlert P, Kurita N, Tanaka H, Kimata M, and Nojiri H 2017 *Phys. Rev. B* **96** 064419
[26] Stock C, Chapon L C, Adamopoulos O, Lappas A, Giot M, Taylor J W, Green M A, Brown C M, and Radaelli P G 2009 *Phys. Rev. Lett.* **103** 077202
[27] Dotsenko V S 1995 *Phys. Usp.* **38** 457
[28] Gaulin B D 1994 *Hyperfine Interact.* **85** 159
[29] Leggett A J 1970 *Phys. Rev. Lett.* **25** 1543
[30] Xiang J, Zhang C, Gao Y, Schmidt W, Schmalzl K, Wang C W, Li B, Xi N, Liu X Y, Jin H, Li G, Shen J, Chen Z, Qi Y, Wan Y, Jin W, Li W, Sun P, and Su G 2024 *Nature* **625** 270
[31] Xu X, Wu Z, Chen Y, Huang Q, Hu Z, Shi X, Du K, Li S, Bian R, Yu R, Cui Y, Zhou H, and Yu W 2025 *Phys. Rev. B* **112** 125163

[32] Sheng J, Wang L, Candini A, Jiang W, Huang L, Xi B, Zhao J, Ge H, Zhao N, Fu Y, Ren J, Yang J, Miao P, Tong X, Yu D, Wang S, Liu Q, Kofu M, Mole R, Biasiol G, Yu D, Zaliznyak I A, Mei J W, and Wu L 2022 *Proc. Natl. Acad. Sci.* **119** e2211193119
[33] Zhu M, Romerio V, Steiger N, Nabi S D, Murai N, Ohira-Kawamura S, Povarov K Y, Skourski Y, Sibille R, Keller L, Yan Z, Gvasaliya S, and Zheludev A 2024 *Phys. Rev. Lett.* **133** 186704
[34] Chen T, Ghasemi A, Zhang J, Shi L, Tagay Z, Chen Y, Chen L, Choi E S, Jaime M, Lee M, Hao Y, Cao H, Winn B, Podlesnyak A A, Pajerowski D M, Zhong R, Xu X, Armitage N P, Cava R, and Broholm C 2024 arXiv:2402.15869 [cond-mat.str-el]
[35] Cui Y, Wu Z, Sun Z, Du K, Luo J, Li S, Yang J, Wang J, Zhou R, Chen Q, Kohama Y, Miyata A, Yang Z, Yu R, and Yu W 2025 arXiv:2509.26151 [cond-mat.str-el]
[36] Singh R R P and Elstner N 1998 *Phys. Rev. Lett.* **81** 4732
[37] Strečka J, Karľová K, Baliha V, and Derzhko O 2018 *Phys. Rev. B* **98** 174426
[38] Chen G V 2024 *Phys. Rev. Lett.* **133** 136703
[39] Zhong R, Guo S, Nguyen L T, and Cava R J 2020 *Phys. Rev. B* **102** 224430
[40] Xu X, Chen T, Wang H, Xie W, Broholm C L, and Cava R J 2024 *Chem. Mater.* **36** 4157
[41] Yue L, Lu Z, Yan K, Wang L, Guo S, Guo R, Chen P, Chen X, and Mei J W 2024 *Phys. Rev. B* **109** 214430
[42] Li Z R, Ouyang Z W, Cao J J, Wang L, Wang Z X, Xia Z C, and Wang J F 2024 *Phys. Rev. B* **109** 224413
[43] Kawamura H 1992 *J. Phys. Soc. Jpn.* **61** 1299
[44] Wu F Y 1982 *Rev. Mod. Phys.* **54** 235
[45] Pomeranchuk I 1950 *Zh. Eksp. Teor. Fiz* **20** 16
[46] Lee D M 1997 *Rev. Mod. Phys.* **69** 645
[47] Richardson R C 1997 *Rev. Mod. Phys.* **69** 683
[48] Chen J L, Fan Z, Zhan B, Hu J, Liu T, Ji J, Wang K, Liao H J, and Xiang T 2025 *Phys. Rev. B* **112** 125130
[49] See Supplemental Material for the crystal structure and magnetic interactions, the low-temperature NMR spectra in the ordered phase, the NMR spectral simulation, the staggered magnetic moments in the UUD phase, and the theoretical modeling and the transition line between the UUD and the supersolid V phase, which include Refs. [41, 42, 50].
[50] Li Z R, Wang L, Cao J J, Dong C, Tian Z M, Wang Z X, Xia Z C, Nojiri H, and Ouyang Z W 2025 *Phys. Rev. B* **112** 094456